

# Comparative study of laminar burning velocity measurement between confined and unconfined spherical flames methods for methane/air and *n*-decane/air premixed flames

R. Le Dortz<sup>1,2</sup>, C. Strozzi<sup>3</sup>, J. Sotton<sup>2</sup>, M. Bellenoue<sup>2</sup>

<sup>1</sup> Safran Tech, Energy and Propulsion Department, Rue des Jeunes Bois, Châteaufort, 78144 Magny-Les-Hameaux, France

<sup>2</sup> Institut Pprime, CNRS, ISAE-ENSMA, Université de Poitiers, F-86962 Futuroscope Chasseneuil, France

<sup>3</sup> Institut Pprime, CNRS, Université de Poitiers, ISAE-ENSMA, F-86962 Futuroscope Chasseneuil, France

## 1 Introduction

The need of measuring laminar burning velocity (LBV) to characterize the fundamental behavior of a premixed flame has involved the development of several experimental methodologies to perform the measurements. One of the most commonly used method is the generation of a spherical flame in closed combustion chamber. The spherical flame, initiated in a homogeneous and quiescent mixture with an electrical discharge deposit, propagates uniformly in overall directions. From this experimental set-up, several authors have defined different methodologies to extract the LBV. These methodologies are mainly separated into two classes: the confined flame and the unconfined flame. In the first one, the LBV is extracted from the pressure signal obtained during combustion process, while in the second one, the LBV is deduced from the visualization of the spherical flame propagation by using the flame radius time-evolution of the flame front. The aim of this study is to compare different methods of LBV measurements with the use of two well-known mixtures: a methane/air premixed flame at normal temperature and pressure (NTP) conditions, and a *n*-decane/air premixed flame at initial temperature  $T_0 = 400$  K and initial pressure  $P_0 = 0.1$  MPa.

## 2 Methodology

### 2.1 Experimental set-up

The spherical combustion chamber employed in this study was already presented during the 26<sup>th</sup> ICDERS meeting [1]. The vessel is a stainless-steel spherical chamber with a 4.2 L inner volume (0.2 m in diameter) and equipped with two UV-sapphire optical access windows (0.07 m in diameter) to ensure optical measurements. This experimental set-up was designed to support pressures up to 10.0 MPa and initial temperatures

up to 470 K. Ignition of the mixture is initiated by an electrical discharge (inductive circuit with plug top coils) of around 20 mJ between two pin-to-pin tungsten electrodes with a 1 mm gap. Pressure during combustion is measured using a piezoelectric dynamic pressure transducer Kistler 6054 AR 0-250 bar coupled with a Kistler ICAM amplifier Type 5073A. The propagation of the flame is recorded using a Schlieren visualization system constituted with a high speed camera Photron FASTCAM SA5 at a frame recording rate of 7 kHz and a collimated LED Opto Engineering as a light source. Frame resolution is 1,024\*1,024 pixels<sup>2</sup> with an exposure time of 4.5  $\mu$ s. Measurements (pressure and recording) are synchronized with the onset of the ignition.

## 2.2 Determination of laminar burning velocity

**From pressure monitoring** First measurements of LBV of spherical flame from pressure signal have been performed by Lewis and Von Elbe in 1934. Starting from the conservation equations and assessing some hypothesis (see [2]), the time evolution of the flame front radius  $R_f$  and the laminar stretch flame speed  $S_u$  can be explained using the temporal evolution of pressure  $P$  and its derivative  $dP/dt$  during combustion:

$$R_f = R_0 \left[ 1 - (1-x) \left( \frac{P_0}{P} \right)^{\frac{1}{\gamma_u}} \right]^{\frac{1}{3}} ; S_u = \frac{R_0}{3} \frac{dx}{dP} \left[ 1 - (1-x) \left( \frac{P_0}{P} \right)^{\frac{1}{\gamma_u}} \right]^{-\frac{2}{3}} \left( \frac{P_0}{P} \right)^{\frac{1}{\gamma_u}} \left( \frac{dP}{dt} \right) \quad (1)$$

where  $R_0$  is the radius of the spherical combustion chamber,  $P_0$  is the initial pressure in the chamber before the combustion process,  $\gamma_u$  is the adiabatic coefficient of fresh gases, and  $x$  is the burnt mass fraction.

Several models exist to formulate the burnt mass fraction  $x$  and its derivative  $dx/dP$  as functions of the time-evolution of pressure during combustion phase. The most common formula was proposed by Lewis and Von Elbe [2] with a linear approach:

$$x = \frac{P - P_0}{P_{ad} - P_0} \quad (2)$$

where  $P_{ad}$  is the adiabatic pressure of combustion. This relation is applicable with the assumption of remaining burnt gas temperature during combustion, and also considering the fresh gas temperature as constant. Thereafter, use of confined method with burnt mass fraction expressed using Eq. (2) is called ‘CV-1’. However, these hypothesis are not valid overall the duration of flame propagation (especially at the end of combustion when heat losses are present). The fresh gases compression by burnt gases increases temperature of reactants. In the same time, the burnt gases temperature will increase due to the pressure rise in the combustion chamber. To solve this problem, Luijten et al. [3] have developed a new accurate model taking into account these temperature evolutions:

$$x = \frac{P - P_0 \cdot f(P)}{P_{ad} - P_0 \cdot f(P)} ; f(P) = \left( \frac{\gamma_b - 1}{\gamma_u - 1} \right) + \left( \frac{\gamma_u - \gamma_b}{\gamma_u - 1} \right) \left( \frac{P}{P_0} \right)^{\frac{\gamma_u - 1}{\gamma_u}} \quad (3)$$

with  $\gamma_b$ , the adiabatic coefficient of burnt gases. This relation is valid overall the duration of flame propagation as long as the front flame is not subject to combustion instabilities which modify the flame front structure, i.e. as long as the flame front remains spherical and adiabatic. Thereafter, use of confined method with burnt mass fraction expressed using Eq. (3) is called ‘CV-2’.

In the light of the continuous variation of equilibrium conditions in burnt gases and the intensity of heat losses by radiation, Van den Bulck [4] and Omari and Tartakovsky [5] recommend the use of a reduced adiabatic coefficient for burnt gases  $\gamma_{br}$  for hydrocarbons defined by the following relation:

$$\gamma_{br} = \frac{1 + \gamma_b}{2} \quad (4)$$

Thereafter, use of confined method with burnt mass fraction expressed using Eq. (3) and with a reduced adiabatic coefficient is called ‘CV-3’.

Other models exist in literature but will not be employed in this work for brevity. From the determination of  $S_u$ , the unstretched LBV  $S_u^0$  is extracting by expressing the flame speed  $S_u$  by the relation:

$$S_u = S_u^0 \left( \frac{T_u}{T_0} \right)^a \left( \frac{P}{P_0} \right)^b \quad (5)$$

where  $T_u$  is the temperature of fresh gases and  $T_0$  is the initial temperature of mixture. In the case of an adiabatic constant volume combustion, the previous equation can be simplified as:

$$S_u = S_u^0 \left( \frac{P}{P_0} \right)^\alpha \quad (6)$$

The unstretched LBV  $S_u^0$  is then deduced by extrapolation between these previous relation and the experimental curve  $S_u = f(P)$  obtained from pressure monitoring in a time duration where instabilities don't take place and where the variation of pressure is high enough to be captured correctly (Fig. 1a).

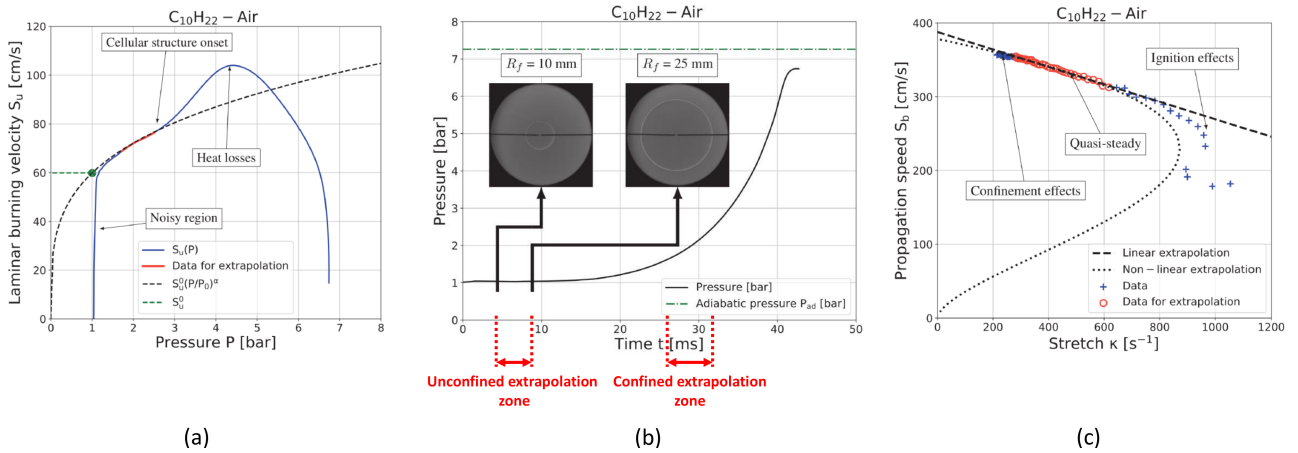


Figure 1: Laminar burning velocities extrapolation determination for (a) confined and (c) unconfined spherical flame techniques; (b) Pressure time-evolution during combustion process

**From flame propagation recording** Extraction of time-evolution for flame front radius, and deduction of propagation speed  $S_b$  and stretch rate  $\kappa = 2S_b/R_F$  [6] can be obtained from the record of flame front propagation by visualization techniques. Markstein [7] have highlighted a linear relation between laminar flame speed  $S_b$  and stretch rate  $\kappa$  for a premixed flame:

$$S_b = S_b^0 - \mathcal{L}_b \kappa \quad (7)$$

where  $\mathcal{L}_b$  is the burnt gases Markstein length which represents sensitivity of the flame front to stretch, and  $S_b^0$  is the unstretched propagation speed.  $S_b^0$  and  $\mathcal{L}_b$  are determined by extrapolation from experimental evolutions of propagation speed  $S_b$  and stretch rate  $\kappa$ . Finally, the unstretched LBV is calculated dividing  $S_b^0$  by the expansion factor  $\sigma$  defined by the ratio of fresh gases density and burnt gases density  $\rho_u/\rho_b$  :

$$S_u^0 = \frac{S_b^0}{\sigma} \quad (8)$$

Thereafter, use of unconfined method with linear relation is called ‘Linear’. Eq. (7) is valid for premixed flame with low stretch, corresponding with LBV near from unstretched LBV. The limits of this model for premixed flames with high stretch were shown in previous studies [8-9]: this model trends to overestimate the unstretched LBV. Instead, use of Kelley and Law non-linear relation [8] is recommended for determining the unstretched LBV:

$$\left(\frac{S_b}{S_b^0}\right)^2 \ln\left(\left(\frac{S_b}{S_b^0}\right)^2\right) = -\frac{2\mathcal{L}_b\kappa}{S_b^0} \quad (9)$$

The relation Eq. (9) have been established using the conservation equations with several assumptions (see [8]). Thereafter, use of unconfined method with non-linear relation is called ‘Non-Linear’. To neglect ignition and confinement effects, extrapolations are performed for radii between  $R_{min} = 10$  mm and  $R_{max} = 25$  mm (Fig. 1b and Fig. 1c).

### 3 Results

This section presents the results of comparison between the different methods. These methods are also compared with the results of numerical determination of unstretched LBV using Cantera chemical code [10] (one-dimensional adiabatic flame propagation) and the chemical kinetic mechanisms GRI-Mech 3.0 [11] and JetSurF 2.0 [12], respectively for methane/air and *n*-decane/air premixed flames. These chemical kinetic mechanisms are known to well represent LBV evolution with equivalence ratio in the retained thermodynamical conditions. Thermodynamic parameters needed for confined and unconfined spherical methods are also evaluated using Cantera and the chemical mechanisms.

#### 3.1 Methane/air premixed flames

Fig. 2a shows the variations of unstretched LBV versus equivalence ratio for the different methods for a methane/air premixed flame at normal temperature and pressure. The methods are able to reproduce the typical trend of LBV curves versus equivalence ratio: the LBV is maximum for a slightly rich mixture and the velocity decreases abruptly as soon as one moves away from this optimum equivalence ratio. Unconfined spherical flames methods seems to give lower velocities in comparison with confined methods.

To have a better visualization of the differences between the methods, relative distance between experimental with the reference numerical results (obtained using Cantera and GRI-Mech 3.0 mechanism) is plotted on Fig. 2b. This comparison shows that deviations between the different spherical flame methods are constant, excepted for the highest equivalence ratios ( $\Phi = 1.3$ ) where the behavior of post-processing methods from pressure monitoring are totally different from those obtained by flame front propagation record. This difference for the highest equivalence ratios had also been observed by Omari [8]. Moreover, it can be noted that results obtained with confined - CV-3 methods are similar to those obtained using unconfined methods.

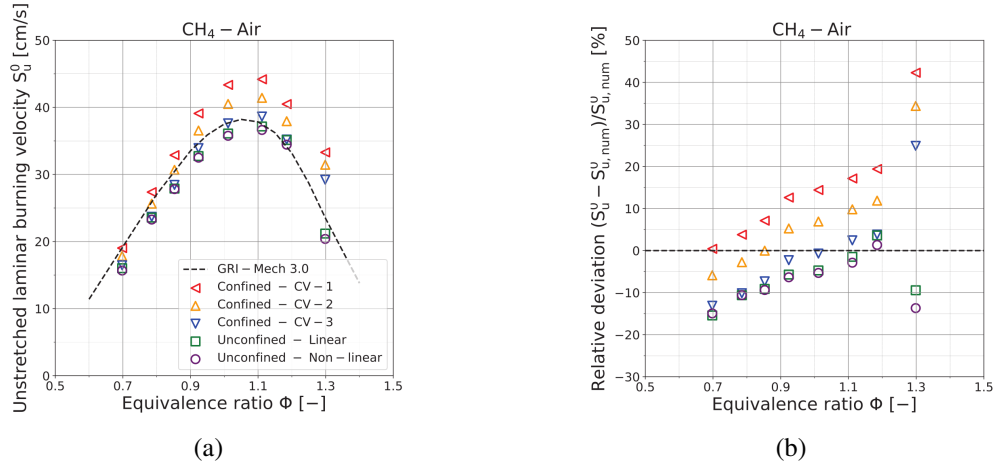


Figure 2: (a) Unstretched laminar burning velocities and (b) Relative deviation plotted versus equivalence ratios for a methane/air premixed flame at initial pressure  $P_0 = 0.1$  MPa and initial temperature  $T_0 = 300$  K

### 3.2 *n*-Decane/air premixed flames

A similar study is performed in this section for a premixed flame of *n*-decane and air at initial temperature  $T_0 = 400$  K and  $P_0 = 0.1$  MPa. The variations of unstretched LBV versus equivalence ratio for different methods are represented on Fig. 3a. As for methane/air premixed flame presented in the previous section, confined spherical flame methods gives higher unstretched LBV than with unconfined spherical flame methods (except for CV-3 method that give the same values as linear method and slightly higher than non-linear method). Concerning confined methods based on the pressure monitoring, LBV have not been evaluated for equivalence ratios higher than 1.15. Indeed, the early-onset of instabilities for low pressure during combustion phenomenon have not allowed the evaluation of the LBV for rich premixed flames of *n*-decane and air at NTP conditions.

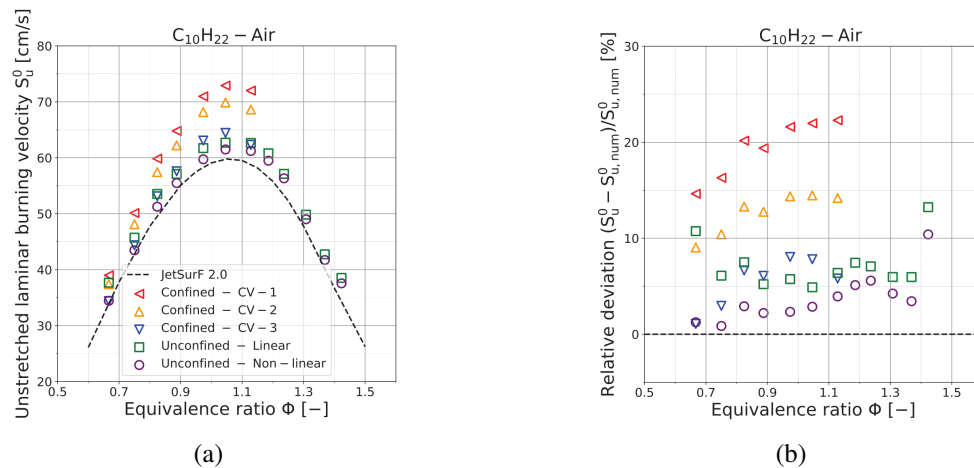


Figure 3: (a) Unstretched laminar burning velocities and (b) Relative deviation plotted versus equivalence ratios for a *n*-decane/air premixed flame at initial pressure  $P_0 = 0.1$  MPa and initial temperature  $T_0 = 400$  K

LBV evaluated from unconfined spherical flame methods are very similar, like for methane/air premixed flames. However, the extrapolation using the linear model of Markstein slightly overestimates the LBV in comparison with the non-linear model of Kelley and Law. This overestimation is due to the assumption of a linear stretch effect, not really reflective of the reality, which has important effects for premixed flames with Lewis number different from unity (it is the case for *n*-decane/air premixed flames). Fig. 3b represents the relative deviation between experimental measurements with the numerical simulation using Cantera and JetSurF 2.0 mechanism as a reference. JetSurF 2.0 mechanism is considered as validated for evaluating the LBV of hydrocarbons and air premixed flames [13]. Unconfined non-linear spherical flame method seems to best represent the numerical results in comparison with the linear method. It is also interesting to underline that the determination of LBV using confined CV-3 method gives also results with a good accuracy (with a maximum relative discrepancy equal to 5.6 % at  $\Phi = 0.97$  between non-linear method and confined CV-3 method), validating this methodology for the panel of tested equivalence ratios for liquid fuels.

## 4 Conclusion

In this study, a comparative analysis of different experimental methodologies for measuring LBV of premixed flames have been realized. These methods have been tested on two cases: methane/air and *n*-decane/air premixed flames. Some deviations have been noted. Especially, comparing with numerical evaluation of LBV, the unconfined method (based on optical post-processing) are able to better reproduce the LBV values. Moreover, results obtained with confined - CV-3 methods are similar to those obtained using unconfined methods.

## Acknowledgements

This work was financially supported by Safran, MBDA and ANR in the framework of the CAPA Chair project on innovative combustion modes for airbreathing propulsion. The authors would also thank E. Mazanchenko for providing her knowledge in experimental support.

## References

- [1] Le Dortz R., Strozzi C., Sotton J. and Bellenoue M. (2017). Effects of Pressure and Temperature on Laminar Burning Velocity of a Kerosene Surrogate, 26<sup>th</sup> ICDERS, Boston (USA).
- [2] Lewis B. and Von Elbe G. (1987). Combustion, Flames and Explosions of Gases.
- [3] Luijten C., Doosje E. and de Goey L. (2009). Accurate analytical models for fractional pressure rise in constant volume combustion, International Journal of Thermal Sciences, 48:1213-1222.
- [4] Van den Bulck E. (2005). Closed algebraic expressions for the adiabatic limit value of the explosion constant in closed volume combustion, Journal of Loss Prevention in the Process Industries, 18:35-42.
- [5] Omari A. and Tartakovsky L. (2016). Measurement of the laminar burning velocity using the confined and unconfined spherical flame methods - A comparative analysis, Comb. Flame 168:127-137.
- [6] Poinso T. and Veynaute D. (2001). Theoretical and numerical combustion.
- [7] Markstein G. (1951). Experimental and theoretical studies of flame-front stability, Journal of the Aeronautical Sciences, 18:199-209.
- [8] Kelley A. and Law. C. (2000) Nonlinear effects in the extraction of laminar flame speeds from expanding spherical flames, Comb. Flame 156:1844-51.
- [9] Chen Z. (2011). On the extraction of laminar flame speed and Markstein length from outwardly propagating flames, Comb. Flame 158:291-300.
- [10] Goodwin D., Moffat H. and Speth R. (2018). Cantera: An object-oriented software toolkit for chemical kinetics, thermodynamics, and transport processes. <https://www.cantera.org>, Version 2.4.0.
- [11] GRI-Mech website.
- [12] Wang H. et al. (2010). A high-temperature chemical kinetic model of *n*-alkane (up to *n*-dodecane), cyclohexane and methyl-, ethyl-, *n*-propyl and *n*-butyl-cyclohexane oxidation at high temperatures. JetSurF version 2.0.
- [13] Comandini A., Dubois T. and Chaumeix N. (2015). Laminar flame speeds of *n*-decane, *n*-butylbenzene, and *n*-propylcyclohexane mixtures. Proc. Comb. Inst. 35:671-678.